

35. M. Holland, C. Bitz, M. Eby, A. Weaver, *J. Climate* **14**, 656 (2001).
36. B. Rudels, *Philos. Trans. R. Soc. London A* **352**, 287 (1995).
37. Y. Kushnir, *J. Climate* **7**, 141 (1994).
38. J. Lean, J. Beer, R. Bradley, *Geophys. Res. Lett.* **22**, 3195 (1995).
39. D. Rind, *J. Geophys. Res.* **103**, 5493 (1998).
40. H. Oeschger, U. Siegenthaler, U. Schotterer, A. Gugler, *Tellus*, **27**, 168 (1975).
41. U. Siegenthaler, *J. Geophys. Res.* **88**, 3599 (1983).
42. O. Marchal, T. F. Stocker, R. Muscheler, *Earth Planet. Sci. Lett.* **185**, 383 (2001).
43. M. Stuiver, T. F. Brazhunas, *Nature* **338**, 405 (1989).
44. R. B. Alley et al., *Geology* **25**, 483 (1997).
45. J. Beer et al., *Nature* **331**, 675 (1988).
46. M. Stuiver, P. Quay, *Science*, **207**, 11 (1980).
47. R. Muscheler, J. Beer, G. Wagner, R. C. Finkel, *Nature* **408**, 567 (2000).
48. G. M. Raisbeck et al., *Mineral. Mag.* **62A**, 1228 (1998).
49. S. R. Epstein, R. Buchsbaum, H. A. Lowenstam, H. C. Urey, *Geol. Soc. Am. Bull.* **64**, 1315 (1953).
50. G. A. Schmidt, G. R. Bigg, E. J. Rohling, 1999. "Global Seawater Oxygen-18 Database" (www.giss.nasa.gov/data/o18data/).
51. U. Pflaumann et al., *Paleoceanography*, in preparation.
52. S. Levitus, R. Gelfeld, *NODC Inventory of Physical Oceanographic Profiles. Key to Oceanographic Records Documentation No. 18* (National Oceanographic Data Center, Washington, DC, 1992).
53. R. Kwok, D. Rothrock, *J. Geophys. Res.* **104**, 5177 (1999).
54. S. J. Johnsen, D. Dahl-Jensen, W. Dansgaard, N. Gundestrup, *Tellus* **47B**, 624 (1995).
55. K. M. Cuffey, G. D. Clow, *J. Geophys. Res.* **102**, 26383 (1997).
56. J. Beer et al., *Nature* **331**, 675 (1988).
57. J. McManus, D. Oppo, L. Keigwin, J. Cullen, G. Bond, *Quat. Res.*, in press.
58. J. McManus et al., *Nature* **371**, 326 (1994).
59. G. Kukla, J. F. McManus, D.-D. Rousseau, I. Chuine, *Quat. Sci. Rev.* **16**, 605 (1997).
60. M. R. Chapman, N. J. Shackleton, *Geology* **27**, 795 (1999).
61. H. Lamb, *Climate, History and the Modern World* (Routledge, London, New York, ed. 2, 1995).
62. D. Dahl-Jensen et al., *Science* **282**, 268 (1998).
63. H. Fischer et al., *Geophys. Res. Lett.* **25**, 1749 (1998).
64. J. Hurrell, Y. Kushnir, M. Visbeck, *Science* **291**, 603 (2001).
65. M. Visbeck, H. Cullen, G. Krahnmann, N. Naik, *Geophys. Res. Lett.* **25**, 4521 (1998).
66. G. Krahnmann, M. Visbeck, G. Reverdin, *J. Phys. Oceanogr.* **31**, 1287 (2001).
67. L. Labeyrie et al., in *Mechanisms of Global Climate Change at Millennial Time Scales*, P. Clark, R. Webb, L. D. Keigwin, Eds. (Geophysical Monograph Series 112, American Geophysical Union, Washington, DC, 1999), pp. 77–98.
68. C. Walebroeck et al., *Paleoceanography* **13**, 272 (1998).
69. J.-C. Duplessy, L. Labeyrie, A. Juillet-Leclerc, J. Duprat, in *The Last Deglaciation: Absolute and Radiocarbon Chronologies*, E. Bard, W. S. Broecker, Eds. (NATO ASI Series I: Global Environmental Change, Springer-Verlag, Berlin, 1992), vol. 2, pp. 201–217.
70. Updated from M. Weinelt, M. Samthein, E. Jansen, H. Erlenkeuser, H. Schulz, in *The Younger Dryas*, S. Troelstra, J. van Hinte, G. M. Ganssen, Eds. (North-Holland, Amsterdam, 1995), pp. 109–115 [M. Weinelt, personal communication; sea-surface temperatures in this publication were estimated with the GLAMP 2000 method (57)].
71. R. Isarin, S. Bohncke, *Quat. Res.* **51**, 158 (1999).
72. L. Keigwin, G. A. Jones, S. Lehman, *J. Geophys. Res.* **96**, 16811 (1991).
73. L. Keigwin, R. Pickart, *Science* **286**, 520 (1999).
74. We thank J. Lynch-Stieglitz, M. Cane, R. Anderson, G. Kukla, J. Lean, and D. Shindell for comments on the manuscript. This work was supported in part by grants from the National Science Foundation and from the National Oceanic and Atmospheric Administration. Support for the core curation facilities of the Lamont-Doherty Earth Observatory (LDEO) Deep-Sea Sample Repository is provided by the National Science Foundation (grant OCE00-02380) and the Office of Naval Research (grant N00014-96-1-0186). This is LDEO contribution 6272.

23 August 2001; accepted 5 November 2001
Published online 15 November 2001;
10.1126/science.1065680
Include this information when citing this paper.

REPORTS

Oscillating Rows of Vortices in Superconductors

T. Matsuda,¹ O. Kamimura,¹ H. Kasai,¹ K. Harada,¹ T. Yoshida,¹
T. Akashi,² A. Tonomura,^{1*} Y. Nakayama,³ J. Shimoyama,³
K. Kishio,³ T. Hanaguri,⁴ K. Kitazawa⁴

Superconductors can be used as dissipation-free electrical conductors as long as vortices are pinned. Vortices in high-temperature superconductors, however, behave anomalously, reflecting the anisotropic layered structure, and can move readily, thus preventing their practical use. Specifically, in a magnetic field tilted toward the layer plane, a special vortex arrangement (chain-lattice state) is formed. Real-time observation of vortices using high-resolution Lorentz microscopy revealed that the images of chain vortices begin to disappear at a much lower temperature, T_d , than the superconducting transition temperature, T_c . We attribute this image disappearance to the longitudinal oscillation of vortices along the chains.

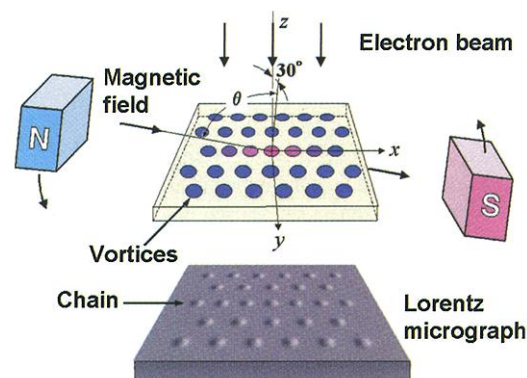
When a magnetic field is applied to a type II superconductor, tiny magnetic vortices, typically arranged in a triangular lattice, form inside it (I) and play a crucial role in the practical use of superconductors as electrical conductors. Unless they are pinned, the vortices begin to flow when driven by an applied current, eventually suppressing superconduc-

tivity. In high-temperature superconductors, however, the vortex behaviors are more complicated because of their anisotropic layered

structure (2). For example, at high temperature T and magnetic field H , a single vortex line can split itself into vortex pancakes in each layer that can be displaced and move independently in a liquid-like state (2–4). In this regime, no pinning occurs and the critical current vanishes. The information about the microscopic behaviors of the vortices is therefore indispensable for developing high-critical current materials.

The effect of the anisotropic layered structures also appears in the static arrangement of vortices. When the field direction is tilted away from the c axis, a triangular vortex-lattice state is transformed into an unconventional arrangement of vortices consisting of alternating domains of linear chains and triangular lattices (5). This phenomenon has recently attracted much attention but has not yet been fully understood, despite both theoretical (6, 7) and experimental (5, 8) investigations.

Fig. 1. Schematic of the experimental setup. A parallel electron beam was incident along the z axis onto a cleaved Bi-2212 thin film at $T = 10$ to 80 K. The film was tilted by 30° around the x axis, and a magnetic field H of 1 to 10 mT was applied to the film. When the electron image was defocused, vortices could be seen as spots of black and white contrasting regions. When the incident angle of the magnetic field direction to the film (θ) was greater than 70° , the vortex arrangement was not a conventional triangular lattice but consisted of alternating domains of linear chains and triangular lattices.



¹Advanced Research Laboratory, Hitachi Ltd., Hatoyama, Saitama 350-0395, Japan. ²Hitachi Instruments Service Co. Ltd., 4-28-8 Yotsuya, Shinjuku-ku, Tokyo 160-0004, Japan. ³Department of Applied Chemistry, University of Tokyo, Tokyo 113-8656, Japan. ⁴Department of Advanced Materials Science, School of Frontier Sciences, University of Tokyo, Tokyo 113-0033, Japan.

*To whom correspondence should be addressed. E-mail: tonomura@harl.hitachi.co.jp

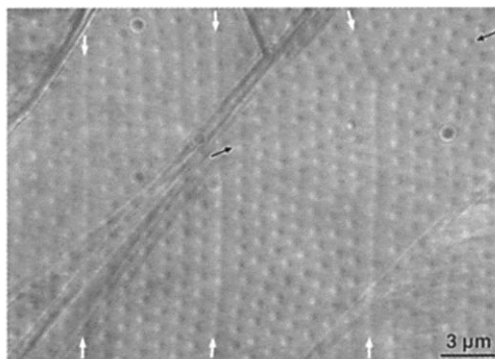
We report findings about the unusual disappearance of the images of chain vortices in $\text{Bi}_2\text{Sr}_2\text{CaCu}_2\text{O}_{8+\delta}$ (Bi-2212) that were found using high-resolution Lorentz microscopy (9, 10), and we explain the results in terms of mobile incommensurate chain vortices surrounded by less mobile commensurate ones. The chain vortices oscillate longitudinally even at temperatures sufficiently low that freezing of the vortex lattices would be expected. The oscillation of chain vortices that begins even at low T is of practical importance because such vortex motion will affect vortex pinning and melting. In addition, our direct observation of incommensurate vortices provides valuable microscopic information about similar phenomena in physical systems such as charge density waves and Josephson junction arrays.

In our experiment (Fig. 1), a 400-nm-thick cleaved single crystal of Bi-2212 was tilted at 30° around the x axis, and an electron beam was incident on the sample from above. A magnetic field H of 1 to 10 mT was applied to the film at incidence angles (θ) of 70° to 90° , and then the sample was cooled down to T in H so that individual vortices in the chain-lattice state could be observed in the out-of-focus plane as Lorentz micrographs.

In the Lorentz micrograph (Fig. 2), the spacing of chain vortices is narrower than, and therefore incommensurate with, that of the surrounding triangular-lattice vortices. The chain vortices appear to be constrained to arrange themselves along these lines. Some of these chains, like the rightmost chain in Fig. 2, appear to terminate or split into two branches when crossing a surface step, as indicated by the dark arrows. However, closer examination shows that the chain did not actually disappear, but only changed direction by bending to the left. Even when the vortex chains were moved by a driving force applied to the vortices by changing H , the line shape was retained even though it was not always straight but curved and changed over time.

Although all the vortex images in the chain-lattice state are clearly observed at low T , the images of some chain vortices begin to disappear when the temperature rises to T_d , which is

Fig. 2. Lorentz micrograph of chain-lattice state of vortices in Bi-2212 film (400 nm thick) at $T = 50$ K, with $B_\perp = 1$ mT and $\theta = 80^\circ$. Three linear chains of vortices can be seen in the vertical direction; they are indicated by the white arrows. Triangular vortex lattices were produced between the chains. The chain direction sometimes changed at the surface steps. The rightmost chain looks as if it may have branched out into two chains in the upper region, but actually did not. This was clarified by observing the chain motion. The chain in the lower region changed direction at the surface step (indicated by two black arrows) and was connected to the left branch in the upper region.



still considerably lower than T_c . The Lorentz micrograph at $T = 70$ K shows three such chains that have disappeared (Fig. 3A). The vortex images of the top and bottom chains have disappeared completely, whereas those of the middle chain are just beginning to disappear.

Why do the images of chain vortices disappear? It is evident from the contrast of the vortex images, which gradually weakens and completely vanishes when T increases, that the vortices themselves do not disappear, but rather the images do. Even among vortices belonging to the same chain, the vortex images are blurred gradually from one place to another, as in the case of the middle chain. Vortices a and b can clearly be seen, but the vortices between them cannot. Such image disappearance must be due to the movement of the vortices, or the spreading out of the magnetic flux of each vortex.

We attribute this vortex-image disappearance to the oscillations of vortices along the chain direction that are too fast to be observed by a detection system with a TV scanning rate. In a triangular lattice, all vortices are commensurate with the underlying potential energy landscape. There is no reason for only one group of vortices to start moving. In a chain-lattice state, however, chains of vortices become incommensurate with the potential distribution. Therefore, only incommensurate chains can move longitudinally at relatively low T , as is known from the theory of commensurate structures (11).

At low enough T , vortices in the equilibrium chain-lattice state receive no forces and therefore do not move. When T increases, however, locally unstable chain vortices such as those located between locally stable vortices a and b in Fig. 3A begin to vibrate back and forth along the chain direction, forming a coupled oscillation (12) (Fig. 3, B and C). As a result, the images of chain vortices partially disappear. At still higher T , the vortex oscillation becomes even stronger and whole chains of vortices begin to disappear, as did the top and bottom chains in Fig. 3A.

The fact that vortices are easy to move in the chain direction is supported by the obser-

vation that the vortices actually move in such a way that some sections of chain vortices reciprocate suddenly and simultaneously along the chain direction. This happens from time to time when the vortex configuration does not completely reach equilibrium, although this movement is not observed under the same conditions of the vortex-image disappearance, but rather under conditions where individual vortices are well separated and their movements can be clearly observed—for example, at B_\perp (normal component of the magnetic flux density) = 0.2 mT, $T = 56$ K, and $\theta = 85^\circ$. Furthermore, chain vortices are predicted to move freely along the chain when they become completely incommensurate (i.e., when the distance between the node vortices a and b increases infinitely). Indeed, we observed such a case

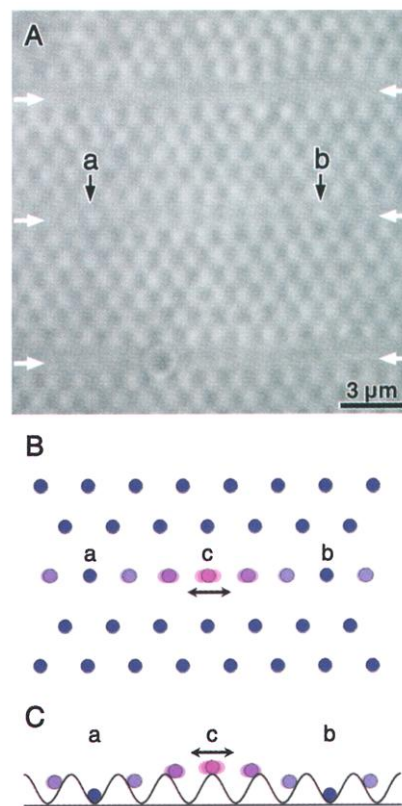


Fig. 3. Disappearing chain vortices. (A) Lorentz micrograph ($T = 70$ K, $B_\perp = 1.2$ mT, $\theta = 80^\circ$): The image of the middle chain partially disappears except for vortices a and b, for example, which are stabilized by the surrounding triangular-lattice vortices. The images of the other two chains disappear along their whole lengths. (B) Vortex arrangement in the chain-lattice state: Red vortices easily oscillate along the chain direction when T increases because their positions are unstable. (C) Vortex arrangement situated on the vortex potential: Vortices a and b are stable while vortex c is unstable and tends to oscillate back and forth in the chain direction as a result of thermal fluctuations. When the distance between a and b becomes infinitely long, chain vortices become incommensurate and can move freely.



Fig. 4. Disappearing images of more vortices in a single chain ($T = 57$ K, $B_{\perp} = 0.8$ mT, $\theta = 80^{\circ}$). We attribute the disappearance of the vortex images to the synchronous oscillation of vortices between the node vortices a and b along the chain direction, just like a coupled oscillation.

where a much larger number of chain vortices disappeared (Fig. 4).

If thermal fluctuations excite the oscillations of chain vortices, the temperature at which the oscillation begins and the vortex image disappears (T_d) must differ depending on the vortex density, because the vortex density changes the spring constant of the chain vortices and also the periodic potential distribution for chain vortices. When we measured T_d as a function of vortex density or B_{\perp} , we found that the T_d values greatly depended on B_{\perp} (Fig. 5). For example, T_d was as low as 20 K when $B_{\perp} = 1.7$ mT, whereas T_d was as high as 70 K when $B_{\perp} = 0.4$ mT.

The tendency for T_d to decrease when B_{\perp} increases can be qualitatively understood as follows: When B_{\perp} increases and the spacing a between vortices becomes narrower, the amplitude of the potential oscillation shown in Fig. 3C decreases as a result of the overlap of each vortex magnetic field. Lowering the potential barrier will naturally make chain vortices start oscillating at lower T . The spring constant k between closer chain vortices increases, thus making it easier for a more rigid incommensurate chain of vortices to slide freely as a whole. This explains why our experimental results show that T_d tends to decrease as B_{\perp} increases (Fig. 5).

We expected to be able to detect the direct indication of the vortex movement at the very beginning of the oscillation under the assumption that vortex lines move as straight rods; hence, we attempted to observe the vortex motion while T gradually increased and crossed T_d . However, the individual vortex images were gradually blurred, and no sign of vortex movement was detected. As a result, our experiments cannot rule out the possibility that a chain vortex line was split into pancake vortices (4) that oscillated in each layer independently for different layers, thus blurring the averaged magnetic field of the vortex line. Even in this case, the partial disappearance of vortex images can be explained because the oscillation of pancake chain vortices in each layer can have the nodes fixed by the surrounding straight vortex lines belonging to the triangular lattices.

The disappearance of the vortex images

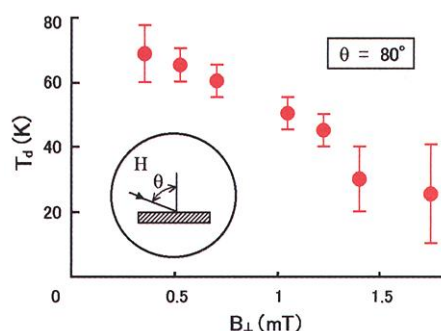


Fig. 5. Disappearance temperature T_d versus magnetic flux density perpendicular to the film B_{\perp} . T_d decreased greatly as B_{\perp} increased. This tendency can be explained by assuming the movement of chain vortices as being that of a coupled oscillation of chain vortices situated on the periodic potential distribution (see Fig. 3C). When vortices are dense (large B_{\perp} and small a), the periodic potential barrier becomes lower as a result of the overlap of the magnetic fields of surrounding triangular vortices, and chain vortices can more easily start oscillating at lower T , thus leading to lower T_d .

may be explained by assuming that the vortex lines are greatly tilted (7). Indeed, the image contrast was shown to decrease when vortex lines were trapped along columnar defects tilted by 70° (13). However, in the present experiment we were able to prove that the observed vortex image disappearance was not attributable to the vortex-line tilting, because the vortex images remained invisible even at a large defocusing distance Δf . The image contrast of tilted vortex lines, which is weak at a relatively short Δf , must become as vis-

ible as that of nontilted vortex lines at greater Δf s (13). Our experiments cannot rule out the possibility that the vortex lines do not simply tilt, but that their magnetic fluxes are somehow blurred in the chain direction (14).

The above discussion may be too simplified and may overlook several features of this phenomenon. For example, the adjacent lines of vortices on both sides of the disappearing vortex chains in Figs. 3A and 4 are not straight; they are slightly bent in such a way that the regions of the disappeared chains are wider at the vortex oscillation and narrower at the oscillation nodes. This may be due to the effect of the locally violent oscillation of vortices.

References and Notes

1. A. A. Abrikosov, *Sov. Phys. JETP* **5**, 1174 (1957).
2. D. J. Bishop, P. L. Gammel, D. A. Huse, C. A. Murray, *Science* **255**, 165 (1992).
3. A. Oral *et al.*, *Phys. Rev. Lett.* **80**, 3610 (1998).
4. J. R. Clem, *Phys. Rev. B* **43**, 7837 (1991).
5. C. A. Bolle *et al.*, *Phys. Rev. Lett.* **66**, 112 (1991).
6. A. I. Buzdin, A. Yu. Simonov, *JETP Lett.* **51**, 191 (1990).
7. A. E. Koshelev, *Phys. Rev. Lett.* **83**, 187 (1999).
8. I. V. Grigorieva, J. W. Steeds, G. Balakrishnan, D. M. Paul, *Physica C* **235-240**, 2705 (1994).
9. K. Harada *et al.*, *Nature* **360**, 51 (1992).
10. T. Kawasaki *et al.*, *Appl. Phys. Lett.* **76**, 1342 (2000).
11. L. M. Floria, J. J. Mazo, *Adv. Phys.* **45**, 505 (1996).
12. C. Reichhardt, C. J. Olson, F. Nori, *Phys. Rev. B* **58**, 6534 (1998).
13. A. Tonomura *et al.*, *Nature* **412**, 620 (2001).
14. More detailed simulations and experiments to pinpoint the cause of the disappearance of chain-vortex images are now in progress (A. Tonomura *et al.*, in preparation).
15. We thank F. Nori, A. Koshelev, T. Hashizume, S. Kagoshima, T. Onogi, P. Gammel, and D. Bishop for their useful suggestions. Supported by SORST, Japan Science and Technology Corporation (JST).

4 September 2001; accepted 1 November 2001

Field-Effect Modulation of the Conductance of Single Molecules

Jan Hendrik Schön,* Hong Meng, Zhenan Bao

Field-effect transistors based on two-component self-assembled monolayers of conjugated and insulating molecules were prepared; the conductance through them can be varied by more than three orders of magnitude by changing the applied gate bias. With very small ratios of conjugated to insulating molecules in the two-component monolayer, devices with only a few "electrically active" molecules can be achieved. At low temperatures, the peak channel conductance is quantized in units of $2e^2/h$ (where e is the electron charge and h is Planck's constant). This behavior is indicative of transistor action in single molecules. On the basis of such single-molecule transistors, inverter circuits with gain are demonstrated.

Modern microelectronics and computation are advancing at an extremely fast rate. At the heart of this field has been the technology of complementary logic metal-oxide semiconductor (CMOS)-based integrated circuits. However, fundamental physical

limitations as well as increasingly prohibitive cost associated with fabrication facilities might slow down further miniaturization of devices to increase computation power within the next couple of decades (1, 2). To continue the trend to ever faster and